Europe PMC Funders Group
Author Manuscript
J Nucl Med. Author manuscript; available in PMC 2021 February 16.

Published in final edited form as:
J Nucl Med. 2018 April 01; 59(4): 625–631. doi:10.2967/jnumed.117.199554.

Cold Kit for Prostate-Specific Membrane Antigen (PSMA) PET Imaging: Phase 1 Study of ^{68}Ga-Tris (Hydroxypyridinone)-PSMA PET/CT in Patients with Prostate Cancer

Michael S. Hofman[1,2], **Peter Eu**[1,2], **Price Jackson**[3], **Emily Hong**[2], **David Binns**[2], **Amir Iravani**[2], **Declan Murphy**[4], **Catherine Mitchell**[5], **Shankar Siva**[1,6], **Rodney J. Hicks**[1,2], **Jennifer D. Young**[7], **Philip J. Blower**[7], **Gregory E. Mullen**[7,8]

[1]Sir Peter MacCallum Department of Oncology, University of Melbourne, Melbourne, Victoria, Australia

[2]Cancer Imaging, Peter MacCallum Cancer Centre, Melbourne, Victoria, Australia

[3]Medical Physics, Peter MacCallum Cancer Centre, Melbourne, Victoria, Australia

[4]Uro-Oncology, Peter MacCallum Cancer Centre, Melbourne, Victoria, Australia

[5]Histopathology, Peter MacCallum Cancer Centre, Melbourne, Victoria, Australia

[6]Radiation Oncology, Peter MacCallum Cancer Centre, Melbourne, Victoria, Australia

[7]Division of Imaging Sciences and Biomedical Engineering, Kings College London, London, United Kingdom

[8]Theragnostics Ltd., Bracknell, United Kingdom

Abstract

^{68}Ga-labeled urea-based inhibitors of the prostate-specific membrane antigen (PSMA), such as ^{68}Ga-labeled *N,N'*-bis(2-hydroxybenzyl)-ethylenediamine-*N,N'*-diacetic acid (HBED)-PSMA-11, are promising small molecules for targeting prostate cancer. A new radiopharmaceutical, ^{68}Ga-labeled tris(hydroxypyridinone) (THP)-PSMA, has a simplified design for single-step kit-based radiolabeling. It features the THP ligand, which forms complexes with $^{68}Ga^{3+}$ rapidly at a low concentration, at room temperature, and over a wide pH range, enabling direct elution from a ^{68}Ge/^{68}Ga generator into a lyophilized radiopharmaceutical kit in 1 step without manipulation. The aim of this phase 1 study was to assess the safety and biodistribution of ^{68}Ga-THP-PSMA.

Correspondence to: Michael S. Hofman.

For correspondence or reprints contact: Michael S. Hofman, Cancer Imaging, Peter MacCallum Cancer Centre, 305 Grattan St., Melbourne, Victoria, Australia 3000. michael.hofman@petermac.org.

Disclosure

The study received funding from Theragnostics Ltd. Philip J. Blower and Gregory E. Mullen are named inventors on patents whose claims encompass the THP chelator. Jennifer D. Young is funded by the King's College London and Imperial College London EPSRC Centre for Doctoral Training in Medical Imaging (EP/L015226/1). We acknowledge support from the KCL and UCL Comprehensive Cancer Imaging Centre funded by CRUK and EPSRC in association with the MRC and DoH (England) and support from the NIRH Biomedical Research Centre awarded to the Guy's and St. Thomas' NHS Foundation Trust in partnership with the King's College London and King's College Hospital NHS Foundation Trust. No other potential conflict of interest relevant to this article was reported.

Europe PMC Funders Author Manuscripts
Europe PMC Funders Author Manuscripts

Europe PMC Funders Author Manuscripts

Methods—Cohort A comprised 8 patients who had proven prostate cancer and were scheduled to undergo prostatectomy; they had Gleason scores of 7–10 and a mean prostate-specific antigen level of 7.8 μg/L (range, 5.4–10.6 μg/L). They underwent PET/CT after the administration of ^{68}Ga-THP-PSMA. All patients proceeded to prostatectomy (7 with pelvic nodal dissection). Dosimetry from multi-time-point PET imaging was performed with OLINDA/EXM. Cohort B comprised 6 patients who had positive ^{68}Ga-HBED-PSMA-11 PET/CT scanning results and underwent comparative ^{68}Ga-THP-PSMA scanning. All patients were monitored for adverse events.

Results—No adverse events occurred. In cohort A, 6 of 8 patients had focal uptake in the prostate (at 2 h: average SUV_{max}, 5.1; range, 2.4–9.2) and correlative 31 staining of prostatectomy specimens on PSMA immunohistochemistry. The 2 ^{68}Ga-THP-PSMA scans with negative results had only 1+1/2+ staining. The mean effective dose was 2.07E-02 mSv/MBq. In cohort B, ^{68}Ga-THP-PSMA had lower physiologic background uptake than ^{68}Ga-HBED-PSMA-11 (in the parotid glands, the mean SUVmax for ^{68}Ga-THP-PSMA was 3.6 [compared with 19.2 for ^{68}Ga-HBED-PSMA-11]; the respective corresponding values in the liver were 2.7 and 6.3, and those in the spleen were 2.7 and 10.5; $P < 0.001$ for all). In 5 of 6 patients, there was concordance in the number of metastases identified with ^{68}Ga-HBED-PSMA-11 and ^{68}Ga-THP-PSMA. Thirteen of 15 nodal abnormalities were subcentimeter. In 22 malignant lesions, the tumor-to-liver contrast with ^{68}Ga-THP-PSMA was similar to that with ^{68}Ga-HBED-PSMA (4.7 and 5.4, respectively; $P = 0.15$), despite a higher SUV_{max} for ^{68}Ga-HBED-PSMA than for ^{68}Ga-THP-PSMA (30.3 and 10.7, respectively; $P < 0.01$).

Conclusion— ^{68}Ga-THP-PSMA is safe and has a favorable biodistribution for clinical imaging. Observed focal uptake in the prostate was localized to PSMA-expressing malignant tissue on histopathology. Metastatic PSMA-avid foci were also visualized with ^{68}Ga-THP-PSMA PET. Single-step production from a Good Manufacturing Practice cold kit may enable rapid adoption.

Keywords

prostate-specific membrane antigen; PET/CT; prostate cancer; ^{68}Ga

Prostate-specific membrane antigen (PSMA) is a highly overexpressed cell surface glycoprotein in prostate cancer (*1–3*). ^{68}Ga-labeled urea-based small molecules that bind with high affinity to the extracellular domain of PSMA, such as ^{68}Ga-labeled N,N-bis(2-hydroxybenzyl)ethylenediamine-N,N’-diacetic acid (HBED)-PSMA-11, have rapidly emerged as a disruptive technology for the imaging of prostate cancer (*4–6*). PET with ^{68}Ga-HBED-PSMA-11 produces high tumor-to-background contrast and has been rapidly adopted in jurisdictions where the regulatory environment enables on-site, extemporaneously compounded radiotracers to be used in clinics. In other jurisdictions, different regulatory requirements have limited the adoption of PSMA PET. Routine clinical production of ^{68}Ga-HBED-PSMA-11 in accordance with Good Manufacturing Practice is limited by synthesis time and the need for an expensive automated synthesis device and on-site radiochemistry expertise.

^{68}Ga-HBED-PSMA-11 PET/CT has demonstrated clinical utility in both initial staging for newly diagnosed patients and restaging for patients in the setting of biochemical recurrence

Europe PMC Funders Author Manuscripts

Europe PMC Funders Author Manuscripts

and has rapidly emerged as a practice-changing modality for the imaging of prostate cancer. More accurate staging for high-risk patients may enable better selection of the most appropriate management strategy and avoid futile locoregional surgery or radiotherapy in patients with metastatic disease. For staging, several studies have demonstrated higher sensitivity of this imaging method than of conventional imaging (*7–10*). In the setting of early biochemical recurrence, PSMA PET/CT has high sensitivity, even in patients with prostate-specific antigen (PSA) levels of less than 1.0 ng/mL, for whom conventional imaging is invariably unhelpful (*11*). PSMA PET/CT can have a consequent high management impact in these patients (*12*).

A new radiopharmaceutical, ^{68}Ga-labeled tris(hydroxypyridi-none) (THP)-PSMA, for the same diagnostic purpose as ^{68}Ga-HBED-PSMA-11 but designed for greatly simplified single-step kit-based radiolabeling, has been developed (*13*). It features the THP ligand, which forms complexes with $^{68}Ga^{3+}$ rapidly at a low concentration, at room temperature, and over a wide pH range. This approach enables elution from a ^{68}Ge/^{68}Ga generator, with low ^{68}Ge breakthrough, into a lyophilized radiopharmaceutical kit in 1 step. Preclinical studies have validated specific binding to PSMA-expressing cells and a biodistribution similar to that of ^{68}Ga-HBED-PSMA-11 (*13*).

The aim of this phase 1 study was to assess the safety and biodistribution of ^{68}Ga-THP-PSMA. The trial hypotheses were that ^{68}Ga-THP-PSMA could be safely administered and that its biodistribution would facilitate specific and sensitive identification of PSMA-expressing malignant tissues using PET/CT, with an acceptable absorbed radiation dose.

Materials and Methods

This investigator-initiated prospective study was sponsored by the Peter MacCallum Cancer Centre, and ethics approval was given by the institutional review board. It was prospectively registered (Australian New Zealand Clinical Trials Registry No. 12615001324505). All subjects gave informed consent.

Fourteen patients with biopsy-proven adenocarcinoma of the prostate were recruited: 8 in cohort A and 6 in cohort B. The safety and biodistribution of ^{68}Ga-THP-PSMA were assessed in all patients. In cohort A, additional aims were to define the whole-body radiation dose and plasma radiotracer clearance and to correlate uptake with tumor PSMA expression on histopathology. In cohort B, an additional aim was to evaluate physiologic and pathologic biodistributions in patients with PSMA-avid malignant disease on ^{68}Ga-HBED-PSMA-11 PET/CT.

Cohort A patients had no prior treatment for prostate carcinoma and were scheduled for prostatectomy. They underwent multiple wholebody PET/CT scans (as detailed later in this article) to determine the biodistribution and dosimetry of ^{68}Ga-THP-PSMA. Regions of interest were drawn around standard organs, and the intensity of uptake was measured using the SUV_{max}. Absorbed organ and whole-body doses were determined by calculation of time–activity values for standard organs using OLINDA/EXM, version 1.1 (*14*).

Europe PMC Funders Author Manuscripts

Europe PMC Funders Author Manuscripts

A positive scan result was defined by visual analysis as uptake in the prostate above background uptake, and uptake was localized using a 4-segment prostate model. The intensity of uptake was measured using the SUV_{max}. Nodal or distant metastases were identified by visual interpretation.

All cohort A patients proceeded to prostatectomy. Samples were fixed in formalin and handled in accordance with routine practice. Sections (3 μm) cut from paraffin blocks containing tumor were immunohistochemically stained for PSMA (Dako [Agilent] clone 3E6; 1:100 dilution) using a Ventana BenchMark ULTRA automated stainer, an incubation period of 32 min, a high-pH epitope retrieval buffer (Ventana Cell Conditioning 1 [CC1] Solution) for 40 min, and a Ventana OptiView Detection Kit (3,3'-diaminobenzidine tetrahydro-chloride-based). PSMA staining was reviewed by a histopathologist with urology subspecialty expertise and scored as absent (0), mild (1+), moderate (2+), or strong (3+); the proportion of tumor cells stained was also recorded. Areas with strong staining for PSMA (31) were considered positive.

For cohort B, the inclusion criteria mandated that patients have prior clinical ^{68}Ga-HBED-PSMA-11 PET/CT demonstrating at least 1 unequivocal PSMA-avid focus considered to represent metastatic prostate cancer. Management did not change between the 2 studies, which were performed within a mean of 12 d (range, 2–22 d). The mean administered activity of ^{68}Ga-HBED-PSMA-11 was 144 MBq (range, 63–205 MBq), and the mean uptake time was 56 min (range, 49–72 min). Patients were imaged on a GE Discovery 690, GE Discovery 710, or Siemens Biograph 64 PET/CT scanner. Details about the ^{68}Ga-THP-PSMA PET/CT acquisition are provided later in this article. Studies were reviewed with masking of the ^{68}Ga-HBED-PSMA-11 findings, and abnormalities in the prostate bed, regional nodes, nonregional nodes, bone metastases, and visceral metastases were enumerated. Tumor-to-liver contrast and SUV_{max} for up to 5 lesions per region were measured on both ^{68}Ga-HBED-PSMA-11 and ^{68}Ga-THP-PSMA.

Formulation of ^{68}Ga-THP-PSMA

Cohort A— ^{68}Ga was eluted from a ^{68}Ge/^{68}Ga generator (iThemba; supplied by IDB Holland bv). Plotting the elution profile of this generator showed that the bulk of the ^{68}Ga eluted with 5 mL of 0.5N HCl in the second milliliter. Accordingly, the generator was first eluted with 1 mL of 0.5N HCl into waste. A second syringe containing 1 mL of 0.5N HCl was then connected to the generator, and the outlet was connected via a hypodermic needle to an appropriately shielded, vented, 40-μg THP-PSMA kit (Theragnostics Ltd.) vial. Radiolabeling was achieved by adding the eluate slowly to the kit vial and diluting the eluate to 5 mL with sterile water for injection. Both needles were then removed, and a sample was taken for the assessment of pH and half-life, thin-layer chromatography, and high-pressure liquid chromatography.

Cohort B—A change in the ^{68}Ge/^{68}Ga generator (Galli Eo; IRE-Elit) for this substudy involved a different radiolabeling method. An evacuated vial (30 mL; GenTech; ANSTO Health) was used to draw approximately 1 mL of the eluate directly from the generator into the THP-PSMA kit vial in accordance with the manufacturer's instructions. Another 4 mL

Europe PMC Funders Author Manuscripts

Europe PMC Funders Author Manuscripts

of 0.1N HCl was added to the kit vial, and all needles were removed. A sample was taken immediately for quality control studies.

Quality Control Studies—A Shimadzu high-pressure liquid chromatography apparatus with both a UV detector (254 nm) and a radiation detector (an Ortec 276 Photomultiplier Base with Preamplifier, Amplifier, Bias Supply and SCA and a Bicron 1 M 11.2 Photomultiplier) was used, along with a Phenomenex Kinetex XB-C18 column (150 × 4.6 mm; 5 μm), an ambient temperature, a flow rate of 1.0 mL/min, and an injection volume of 100 μL. Approximate retention times under these conditions were 1.5 min for ^{68}Ga, 12.0 min for THP-PSMA, and 14.0 min for ^{68}Ga-THP-PSMA. The mobile phase was trifluoroacetic acid:water:acetonitrile (0.05:90:10).

For thin-layer chromatography, Varian iTLC-SG SGI0001 strips were used with a mobile phase of 7.7% (w/v) ammonium acetate: methanol (50:50) and a spot volume of 5 μL. The approximate R_f values were 0.0 for colloidal ^{68}Ga, 0.0 for free unbound ^{68}Ga, and 1.0 for ^{68}Ga-THP-PSMA. The pH was 6–7. The radiochemical yield and purity (activity of ^{68}Ga-THP-PSMA as a percentage of total $^{68}Ga^{3+}$ activity) were greater than 99%. ^{68}Ge breakthrough determined by half-life measurement was less than 0.001% for both generators.

Dose and Activity Administered—The mean administered mass of THP-PSMA was 35 μg (SD, 10%; range, 32–38 μg). The mean administered activities of ^{68}Ga were 238 MBq (range, 228–270 MBq) for cohort A and 232 MBq (range, 172–275 MBq) for cohort B.

PET/CT Imaging

Images were acquired on a GE Discovery 690 PET/CT device incorporating time-of-flight. Acquisition protocols are summarized in Figure 1. Cohort A patients underwent repeated imaging for 90 min (single low-dose CT followed by 7 acquisitions from vertex to upper thighs; 1 min per bed step). Two further acquisitions were performed at 2 and 3 h after injection (each with ultra-low-dose CT; 1.5 and 2 min per bed step).

For cohort B patients, PET/CT imaging was performed at 15, 60, and 120 min from vertex to upper thighs with ultra-low-dose CT at 15 and 120 min and low-dose CT at 60 min. Patients were asked to void their bladder before the 60- and 120-min images.

Plasma Sampling—In cohort A, venous blood samples (5 mL) were taken at 5, 10, 20, 40, 60, 90, 120, and 180 min. From each sample, 2 mL were taken with a pipette for ^{68}Ga counting (Biodex 950 Well Counter; Biodex Medical Systems).

Safety Monitoring—All patients were monitored for adverse events from the time of ^{68}Ga-THP-PSMA administration for 24 h. Before injection, baseline electrocardiogram, hematology, biochemistry assay, and clotting measurements were obtained. Vital signs (blood pressure, heart rate, temperature, and oxygen saturation) were recorded every 15 min for 3 h. Blood tests were repeated at 24 h, and the patient was contacted by a clinician, in person or by telephone, to document any adverse events. Any adverse event was assessed for severity according to the Common Terminology Criteria for Adverse Events (CTCAE), v4.0,

Europe PMC Funders Author Manuscripts

Europe PMC Funders Author Manuscripts

manual (https://www.eortc.be/services/doc/ctc/CTCAE_4.03_2010-06-14_QuickReference_5x7.pdf).

Statistical Considerations—The number of patients was a pragmatic sample size for a safety study. Data analysis was descriptive. In cohort B, the uptake of ^{68}Ga-THP-PSMA and that of ^{68}Ga-HBED-PSMA were compared using a paired *t* test.

Results

Fourteen patients were screened, and all proceeded to study participation and completion. No adverse events attributed to ^{68}Ga-THP-PSMA administration were recorded in any of the patients.

Cohort A

Baseline cohort characteristics and results are summarized in Table 1. Six of 8 patients had uptake in the prostate higher than background uptake. The SUV_{max} of a dominant prostate abnormality at 120 min was 5.1 (range, 2.4–9.2). The earlier-time-point acquisitions obtained for the purpose of dosimetry calculation were not suitable for the determination of prostate uptake because of a single CT acquisition at 0 min and subsequent bladder filling, which resulted in an attenuation correction artifact in the surrounding pelvis.

Physiologic uptake was seen in the lacrimal glands, salivary glands, liver, spleen, and duodenum. The intensity of uptake in these organs was low (Table 2). High kidney, ureter, and bladder activities were seen because of renal excretion.

The mean effective dose was 2.07E–02 mSv/MBq (Table 3). Because patients were asked not to void during the imaging period and bladder accumulation occurred, this dose represents an overestimate of that used in routine clinical practice. Plasma clearance was measured in 7 patients; technical difficulties obviated measurement in 1 patient. The findings were consistent; all patients showed 2-phase exponential clearance, with a mean first-phase half-time of 5.9 min (range, 2.6–8.4 min) and a second-phase half-time of 91.1 min (range, 67.2–118.5 min) (Fig. 2).

All patients proceeded to prostatectomy. PSMA immunohistochemistry staining with an intensity of 3+ was seen in 6 THP-PSMA scans with positive results, and 1+/2+ staining was seen in the 2 THP-PSMA scans with negative results (Fig. 3). Seven of 8 patients underwent pelvic nodal dissection. Pathologic pelvic nodal involvement was identified in 2 patients without a corresponding ^{68}Ga-THP-PSMA abnormality, although the involved nodes were both smaller than 1 mm, a size well below the imaging resolution. One patient had focal intense uptake in subcentimeter pelvic nodes without a pathologic abnormality. Follow-up at 6 mo confirmed the accuracy of the initial ^{68}Ga-THP-PSMA PET findings with rising PSA levels, ^{68}Ga-HBED-PSMA-11 findings, and contrast-enhanced CT confirming nodal progression (Fig. 4).

Europe PMC Funders Author Manuscripts

Europe PMC Funders Author Manuscripts

Cohort B

Imaging at 60 min showed that ^{68}Ga-THP-PSMA had lower background physiologic uptake in salivary glands, liver, and spleen than ^{68}Ga-HBED-PSMA-11 (in the parotid glands, the mean SUV_{max} for ^{68}Ga-THP-PSMA was 3.6 [compared with 19.2 for ^{68}Ga-HBED-PSMA-11]; the respective corresponding values for the liver were 2.7 and 6.3, and those for the spleen were 2.7 and 10.5; $P < 0.001$ for all). In all 6 patients, metastatic lesions were identified on both HBED-PSMA and THP-PSMA (Table 4; Figs. 5 and 6). In the lesion analysis, a total of 22 malignant lesions were measured (15 lymph node, 6 bone, and 1 prostate). On correlative CT, 13 of 15 nodes were smaller than 1 cm in the short-axis diameter; the means were 9.9 mm in the long axis (range, 5–17 mm) and 7.2 mm in the short axis (range, 3–15 mm). In 5 of 6 patients, there was concordance in the numbers of metastases identified on ^{68}Ga-HBED-PSMA-11 and ^{68}Ga-THP-PSMA. In the lesion analysis, the tumor-to-liver contrast ratios were not different between the 2 radiotracers, with means of 5.4 for ^{68}Ga-HBED-PSMA and 4.7 for ^{68}Ga-THP-PSMA ($P = 0.15$). The absolute SUV_{max} was significantly higher on ^{68}Ga-HBED-PSMA, with a mean of 30.3, than on ^{68}Ga-THP-PSMA, with a mean of 10.7 ($P < 0.01$). In 1 patient, 4 abnormal foci were identified on ^{68}Ga-HBED-PSMA PET, and 2 were identified on ^{68}Ga-THP-PSMA PET; the 2 lesions identified only on ^{68}Ga-HBED-PSMA PET were in the prostate and a 3-mm internal iliac node. No further follow-up was available to validate the findings. There was no management change in this patient because of the difference in the 2 scans.

Discussion

In the present study, we provided first-in-man validation of ^{68}Ga-THP-PSMA, the first clinical tracer to use the novel THP chelator, enabling labeling in less than 5 min at room temperature. The DOTA chelator incorporated in the widely used DOTATATE requires pH adjustment, heating followed by cooling, and sometimes a purification step, necessitating either significant manual handling or the use of an automated synthesis device. These factors increase expenses and may not be compliant with Good Manufacturing Practice. Moreover, cartridge-based automated synthesis typically takes more than 30 min, which is suboptimal for a short-life radionuclide such as ^{68}Ga. HBED chelation can be performed at room temperature, but this approach produces a mixture of *cis/trans* geometric isomers (*5*). Recently, favorable labeling properties for the DATA chelator for labeling DATATOC in a kit formulation were described (*15*). THP-PSMA was developed as a single-step Good Manufacturing Practice radiopharmaceutical kit, requiring only the addition of an unprocessed, unfractionated generator eluate to a single vial. Depending on the generator used, however, additional simple steps may be required. The single-step kit can also be used with generators with less than 0.001% ^{68}Ge breakthrough and an appropriate elution volume, such as the GalliaPharm Generator (Eckert & Ziegler) (7).

^{68}Ga-THP-PSMA provides low absorbed doses and effective doses similar to those published for ^{68}Ga-HBED-PSMA-11 (*16*). In the present study, a mean effective dose of 4.9 mSv was observed. However, recently published ^{68}Ga-PSMA-11 guidelines recommended 1.8–2.2 MBq/kg of body weight (*17*), which would result in an exposure to 2.4–2.9 mSv from the PET component with ^{68}Ga-THP-PSMA. This exposure is significantly lower than

Europe PMC Funders Author Manuscripts

Europe PMC Funders Author Manuscripts

those obtained with other imaging tests typically used for the imaging of prostate cancer, such as ^{18}F-fluorocholine, ^{18}F-FDG, bone scintigraphy, and dedicated contrast-enhanced CT.

^{68}Ga-THP-PSMA had significantly lower background physiologic uptake than ^{68}Ga-HBED-PSMA-11. Specifically, salivary and tear gland (lacrimal, parotid, and submandibular), liver, and small bowel uptake was significantly lower. The mechanism of uptake in the salivary glands remains uncertain, perhaps reflecting nonspecific radiotracer excretion, PSMA expression in these tissues, or an unknown target with similar recognition properties. Because there is no known expression of PSMA in the liver or spleen, the differential uptake may reflect particulate radioactivity with ^{68}Ga, which is known to generate colloidal ^{68}Ga between pHs 3 and 7. The tumor-to-liver contrast observed with ^{68}Ga-THP-PSMA-11 was similar to that observed with ^{68}Ga-HBED-PSMA despite absolute uptake being lower. Subcentimeter abnormalities were frequently visualized, reinforcing the high sensitivity of PSMA PET imaging.

Conclusion

^{68}Ga-THP-PSMA can be manufactured quickly using a generator and a cold-kit vial, analogous to procedures widely used for ^{99m}Tc radiotracer production. ^{68}Ga-THP-PSMA can be safely administered, with absorbed radiation doses of less than 3 mSv from the PET component. Focal uptake in the prostate correlates with histopathologic PSMA expression. Background physiologic uptake was significantly lower with ^{68}Ga-THP-PSMA than with ^{68}Ga-HBED-PSMA. Subcentimeter metastases were frequently identified with both radiotracers, with similar tumor-to-liver contrast despite lower absolute uptake with ^{68}Ga-THP-PSMA.

Acknowledgments

We thank the clinical trials coordinator, Elizabeth Drummond, for conducting the trial and the patients for their participation.

References

1. Ghosh A, Heston WD. Tumor target prostate specific membrane antigen (PSMA) and its regulation in prostate cancer. J Cell Biochem. 2004; 91:528–539. [PubMed: 14755683]
2. Silver DA, Pellicer I, Fair WR, Heston WD, Cordon-Cardo C. Prostate-specific membrane antigen expression in normal and malignant human tissues. Clin Cancer Res. 1997; 3:81–85. [PubMed: 9815541]
3. Wright GL Jr, Haley C, Beckett ML, Schellhammer PF. Expression of prostate-specific membrane antigen in normal, benign, and malignant prostate tissues. Urol Oncol. 1995; 1:18–28. [PubMed: 21224086]
4. Schäfer M, Bauder-Wüst U, Leotta K, et al. A dimerized urea-based inhibitor of the prostate-specific membrane antigen for ^{68}Ga-PET imaging of prostate cancer. EJNMMI Res. 2012; 2:23. [PubMed: 22673157]
5. Eder M, Schäfer M, Bauder-Wüst U, et al. ^{68}Gacomplex lipophilicity and the targeting property of a urea-based PSMA inhibitor for PET imaging. Bioconjug Chem. 2012; 23:688–697. [PubMed: 22369515]

Europe PMC Funders Author Manuscripts

6. Afshar-Oromieh A, Malcher A, Eder M, et al. PET imaging with a [^{68}Ga]gallium-labelled PSMA ligand for the diagnosis of prostate cancer: biodistribution in humans and first evaluation of tumour lesions. Eur J Nucl Med Mol Imaging. 2013; 40:486–95. [PubMed: 23179945]
7. Maurer T, Gschwend JE, Rauscher I, et al. Diagnostic efficacy of ^{68}gallium-PSMA positron emission tomography compared to conventional imaging for lymph node staging of 130 consecutive patients with intermediate to high risk prostate cancer. J Urol. 2016; 195:1436–1443. [PubMed: 26682756]
8. Budaus L, Leyh-Bannurah SR, Salomon G, et al. Initial experience of ^{68}Ga-PSMA PET/CT imaging in high-risk prostate cancer patients prior to radical prostatectomy. Eur Urol. 2016; 69:393–396. [PubMed: 26116958]
9. Herlemann A, Wenter V, Kretschmer A, et al. ^{68}Ga-PSMA positron emission tomog-raphy/computed tomography provides accurate staging of lymph node regions prior to lymph node dissection in patients with prostate cancer. Eur Urol. 2016; 70:553–557. [PubMed: 26810345]
10. van Leeuwen PJ, Emmett L, Ho B, et al. Prospective evaluation of ^{68}gallium-prostate-specific membrane antigen positron emission tomography/computed tomography for preoperative lymph node staging in prostate cancer. BJU Int. 2017; 119:209–215. [PubMed: 27207581]
11. Perera M, Papa N, Christidis D, et al. Sensitivity, specificity, and predictors of positive ^{68}Ga-prostate-specific membrane antigen positron emission tomography in advanced prostate cancer: a systematic review and meta-analysis. Eur Urol. 2016; 70:926–937. [PubMed: 27363387]
12. van Leeuwen PJ, Stricker P, Hruby G, et al. ^{68}Ga-PSMA has a high detection rate of prostate cancer recurrence outside the prostatic fossa in patients being considered for salvage radiation treatment. BJU Int. 2016; 117:732–739. [PubMed: 26683282]
13. Young JD, Abbate V, Imberti C, et al. ^{68}Ga-THP-PSMA: a PET imaging agent for prostate cancer offering rapid, room-temperature, 1-step kit-based radiolabeling. J Nucl Med. 2017; 58:1270–1277. [PubMed: 28408532]
14. Stabin MG, Sparks RB, Crowe E. OLINDA/EXM: the second-generation personal computer software for internal dose assessment in nuclear medicine. J Nucl Med. 2005; 46:1023–1027. [PubMed: 15937315]
15. Seemann J, Waldron B, Parker D, Roesch F. DATATOC: a novel conjugate for kit-type ^{68}Ga labelling of TOC at ambient temperature. EJNMMI Radiopharmacy and Chemistry. 2016; 1:4. [PubMed: 29564381]
16. Pfob CH, Ziegler S, Graner FP, et al. Biodistribution and radiation dosimetry of ^{68}Ga-PSMA HBED CC: a PSMA specific probe for PET imaging of prostate cancer. Eur J Nucl Med Mol Imaging. 2016; 43:1962–1970. [PubMed: 27207281]
17. Fendler WP, Eiber M, Beheshti M, et al. ^{68}Ga-PSMA PET/CT: joint EANM and SNMMI procedure guideline for prostate cancer imaging—version 1.0. Eur J Nucl Med Mol Imaging. 2017; 44:1014–1024. [PubMed: 28283702]

Europe PMC Funders Author Manuscripts

Europe PMC Funders Author Manuscripts

Europe PMC Funders Author Manuscripts

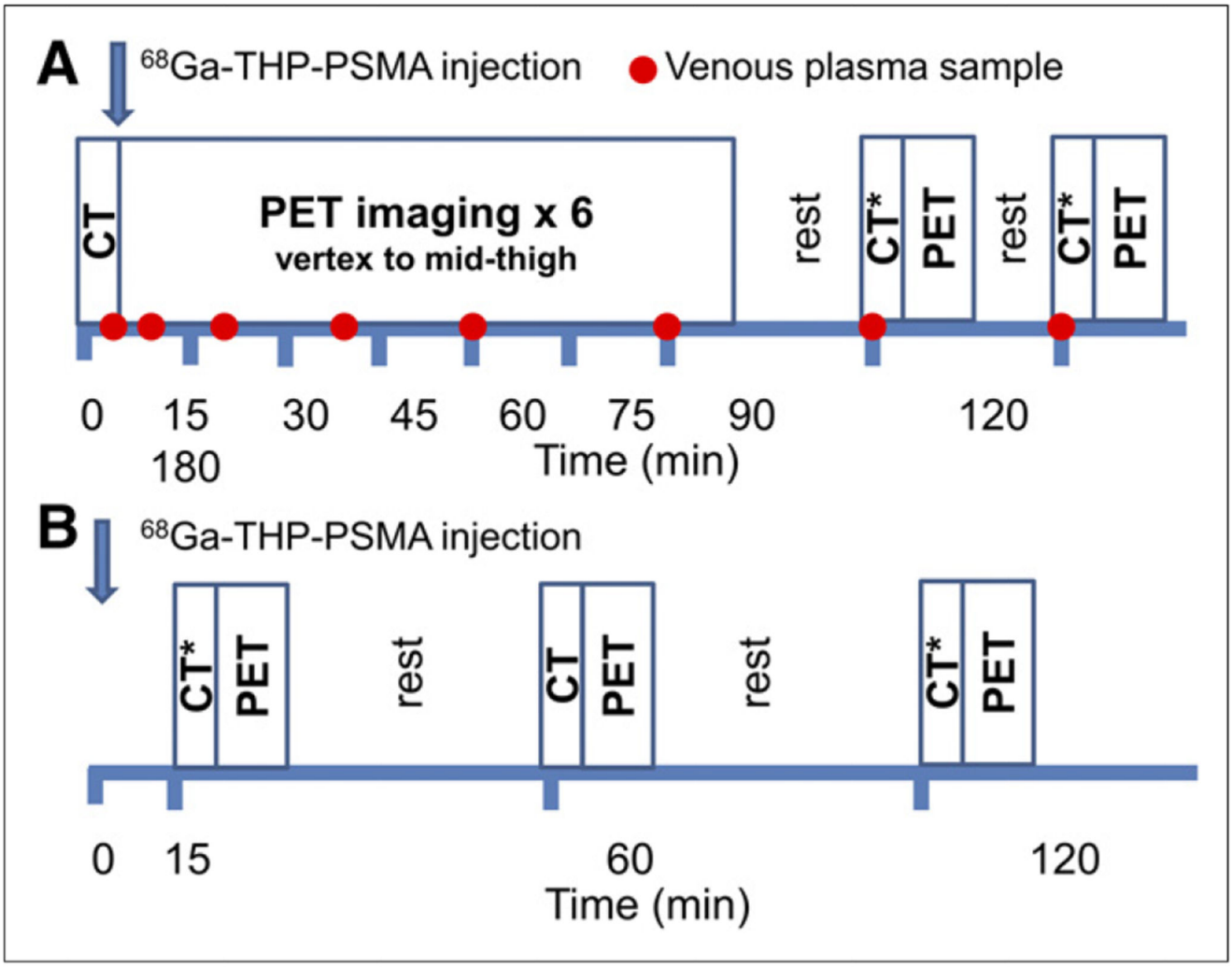

Figure 1. Summary of PET/CT acquisition protocol for cohort A (A) and cohort B (B).
*Ultra-low-dose CT for attenuation correction.

Europe PMC Funders Author Manuscripts

Europe PMC Funders Author Manuscripts

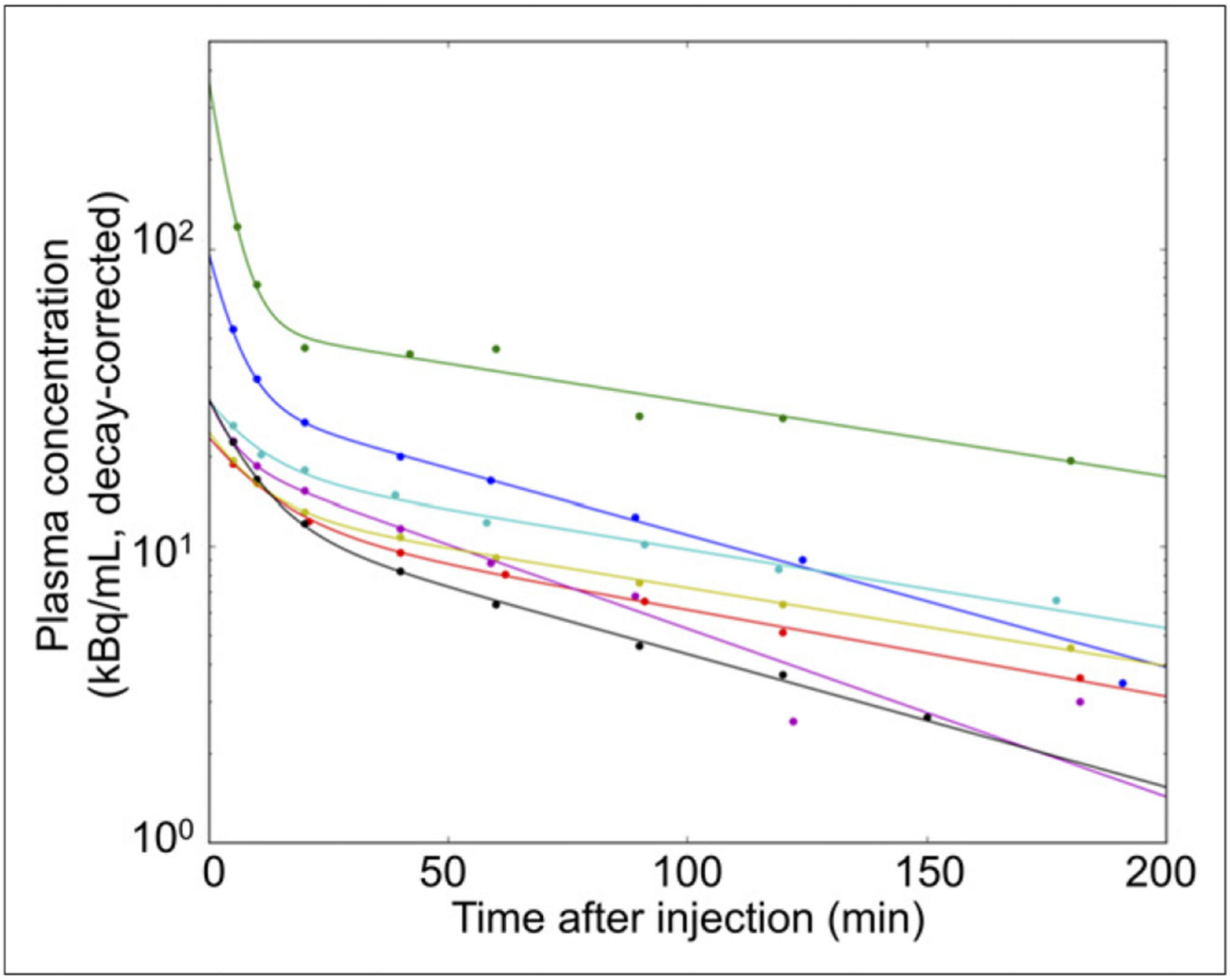

Figure 2. Plasma clearance of ^{68}Ga-THP-PSMA.
Different colors represent different patients.

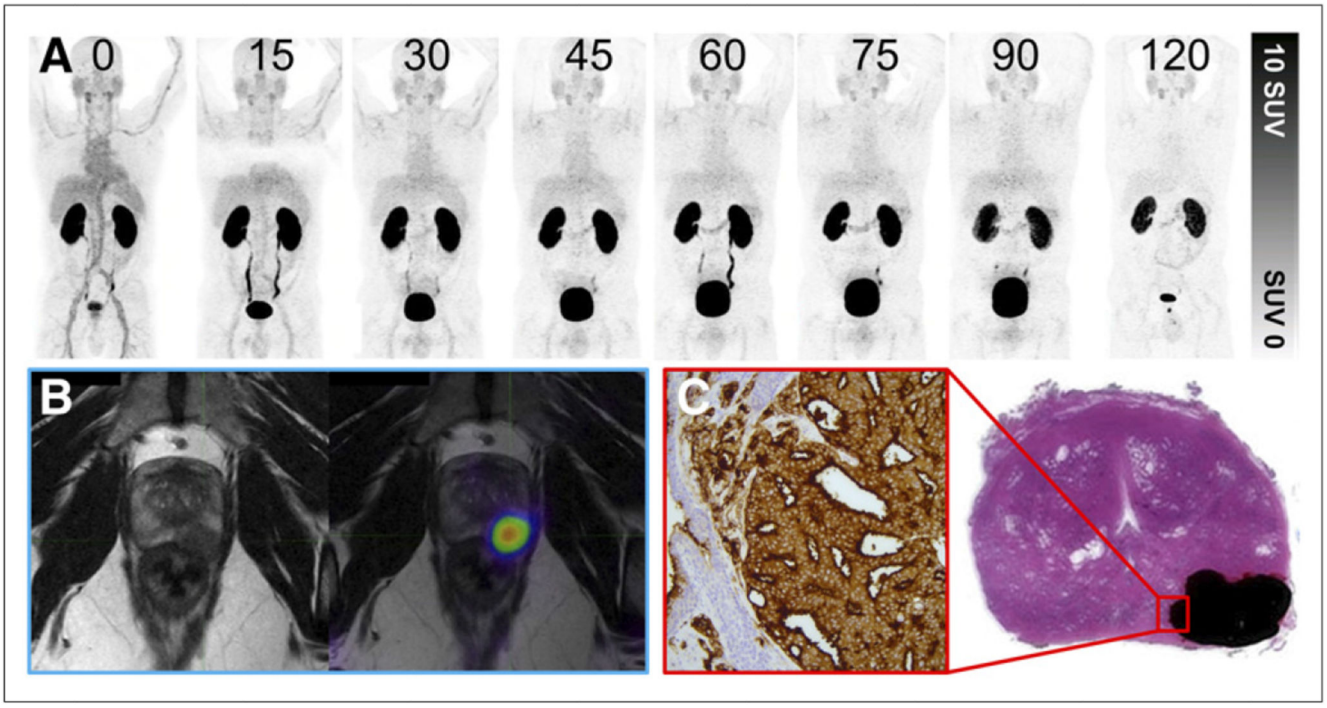

Figure 3. Patient with prostate adenocarcinoma with Gleason score of 4 + 4 = 8 and PIRADS 5 on prior multiparametric MRI.

(A) ^{68}Ga-THP-PSMA PET multi-time-point images (0–120 min) demonstrating rapid blood-pool clearance and low background activity. (B) PET image (120 min) after voiding fused to MRI T2-weighted sequence. Focal uptake can be seen in left posterior midzone lesion. (C) Histopathologic correlation after prostatectomy. Area of adenocarcinoma is shaded in black; magnified area demonstrates 3+ staining on PSMA immunohistochemistry.

Europe PMC Funders Author Manuscripts
Europe PMC Funders Author Manuscripts

Europe PMC Funders Author Manuscripts

Europe PMC Funders Author Manuscripts

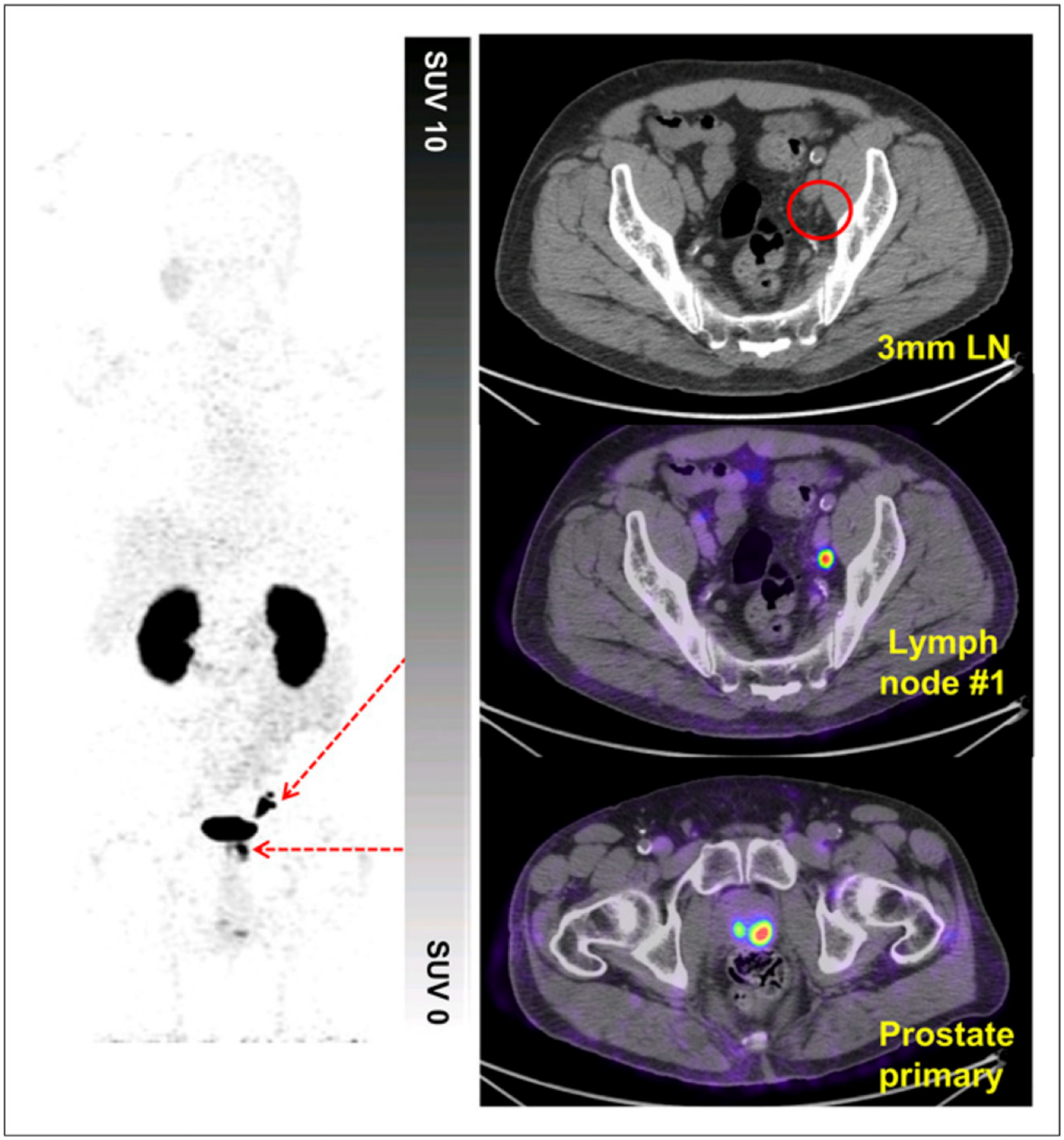

Figure 4. Patient with prostate adenocarcinoma with Gleason score of 4 + 5 = 9.

High uptake can be seen in primary prostate tumor, and focal uptake can be seen in several left external iliac lymph nodes (LN) of <5 mm (120-min image). Patient proceeded to prostatectomy and pelvic nodal clearance. Pathologic staging demonstrated no nodal involvement (pN0 staging). Follow-up demonstrated persistently elevated and rising PSA levels; repeat imaging at 6 mo confirmed presence and progression of baseline ^{68}Ga-THP-PSMA PET/CT findings. pN0 staging therefore was interpreted as false-negative because of sampling error.

Europe PMC Funders Author Manuscripts

Europe PMC Funders Author Manuscripts

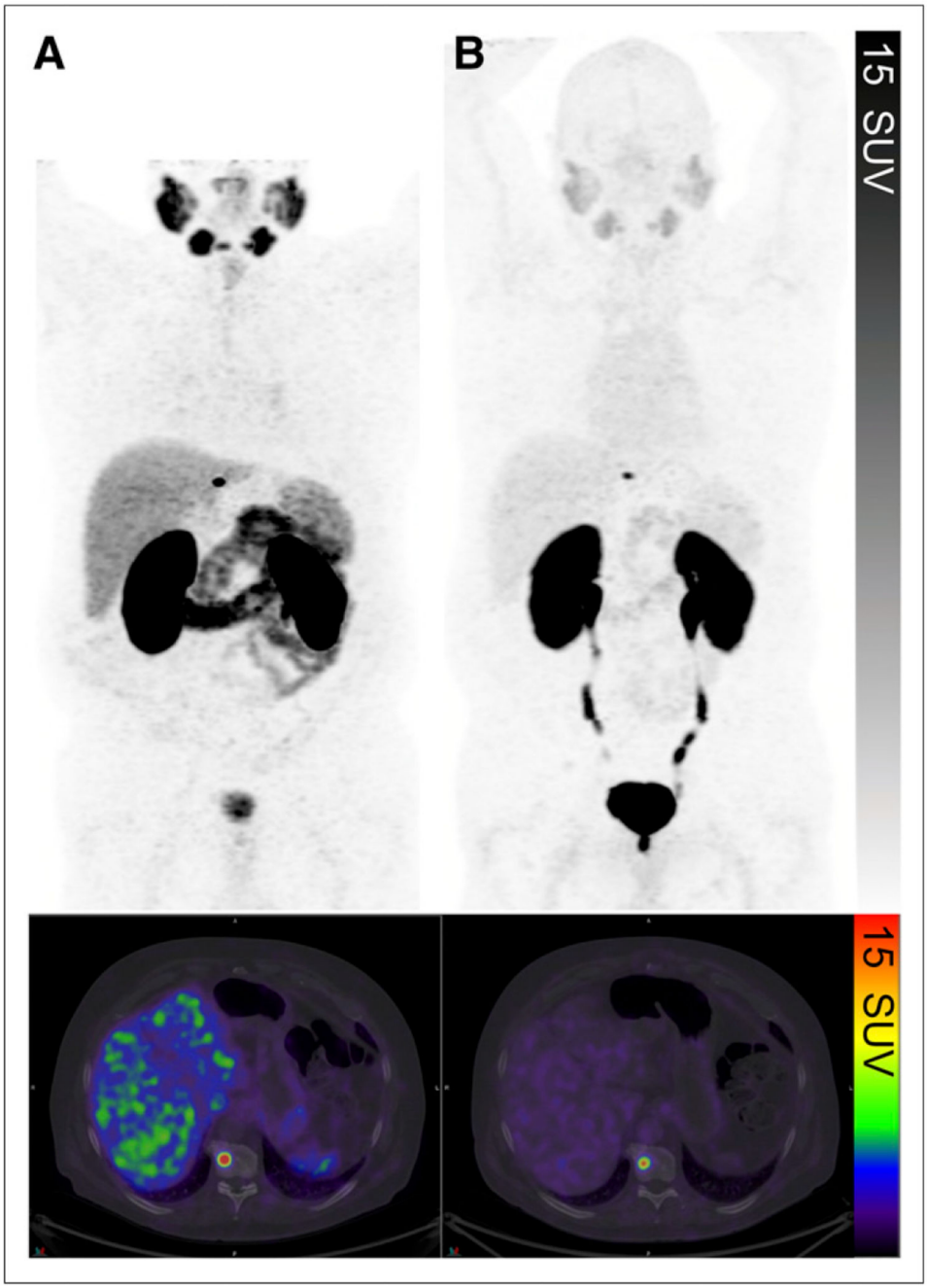

Figure 5. Comparison of ^{68}Ga-HBED-PSMA PET/CT (177 MBq; 56min uptake period) (A) and ^{68}Ga-THP-PSMA PET/CT (232 MBq; 60-min uptake period) (B) in same patient. Solitary focal intense abnormality in T10 vertebral body was well visualized on both. Lower background physiologic uptake can be seen on ^{68}Ga-THP-PSMA study.

Europe PMC Funders Author Manuscripts

Europe PMC Funders Author Manuscripts

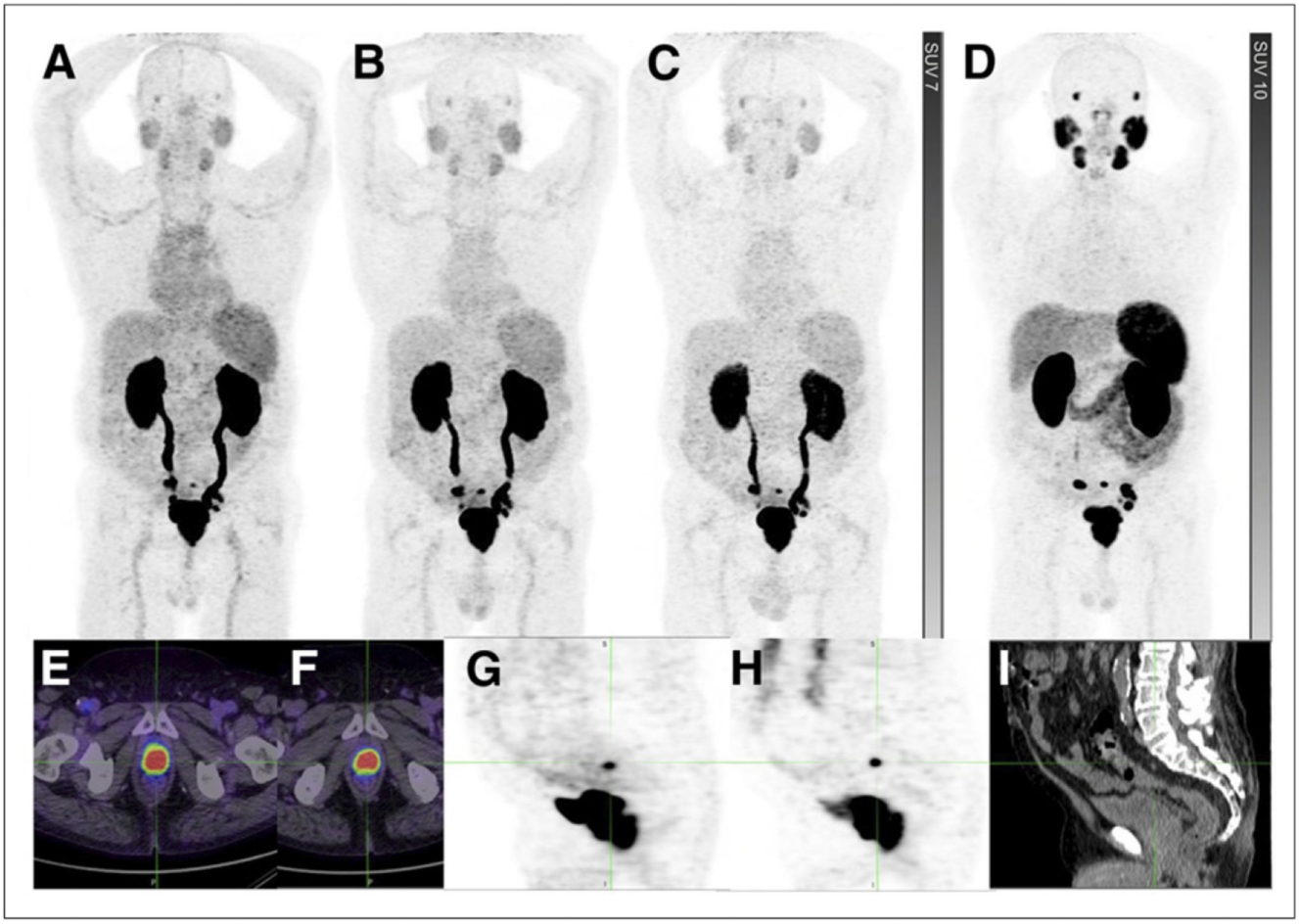

Figure 6. Primary staging for patient with prostate adenocarcinoma with Gleason score of 5 + 4 = 9 and normal conventional imaging.

(A-D) Comparison of ^{68}Ga-THP-PSMA maximum-intensity-projection (MIP) images at 15 min (A), 60 min (B), and 120 min (C) and ^{68}Ga-HBED-PSMA MIP image at 60 min (D). (E and F) Focal intense uptake in primary prostate tumor on ^{68}Ga-THP-PSMA PET/CT (E) and ^{68}Ga-HBED-PSMA PET/CT (F). Multiple subcentimeter pelvic nodal metastases were visualized. (G-I) Focal uptake on ^{68}Ga-THP-PSMA (G) and ^{68}Ga-PSMA-PSMA (H), corresponding to presacral node of <5 mm on CT (I).

Europe PMC Funders Author Manuscripts

Europe PMC Funders Author Manuscripts

Table 1
Baseline Characteristics and Results for Cohort A

		Preoperative data				^{68}Ga-THP-PSMA		Postoperative data		
Patient	Age (y)	Gleason score (GS)	PSA	Clinical T stage	MRI	Prostate SUV_{max}	Nodal SUV_{max}	GS	Pathologic stage	PSMA IHC
1	71	3 + 5 = 8	10.3	T3	PIRADS 4	5.6		4 + 3 = 7	T3bN1[*]	3+
2	64	3 + 4 = 7	6.2	T2a/b	PIRADS 5			3 + 4 = 7	T2cNx	2+
3	55	4 + 3 = 7	9.6	T1c	PIRADS 2	2.5		4 + 3 = 7	T3aN0	3+
4	65	3 + 4 = 7	5.4	T1	PIRADS 4	4.0		3 + 4 = 7	T2cNx	3+
5	71	3 + 4 = 7	3.2	T2b	PIRADS 5	2.4		4 + 3 = 7	T3aNx	3+
6	54	5 + 5 = 10	9	T2b	PIRADS 5			4 + 5 = 9	T3aN1[†]	1+
7	46	4 + 4 = 8	10.6	T3a	PIRADS 5	7.1		4 + 5 = 9	T3aN0	3+
8	58	4 + 4 = 8	8	T2c	Not performed	9.2	18.4[‡]	4 + 5 = 9	T3bN0	3+

[*] 0.6 mm in 1 lymph node.

[†] 0.1 mm in 1 lymph node.

[‡] Confirmed as true-positive on follow-up, with sampling error resulting in pathologic N0 staging.

IHC = immunohistochemistry; PIRADS = Prostate Imaging Reporting and Data System, v2.

Europe PMC Funders Author Manuscripts

Europe PMC Funders Author Manuscripts

Table 2

Physiologic Uptake of ^{68}Ga-THP-PSMA and ^{8}Ga-HBED-PSMA

		^{68}Ga-THP-PSMA uptake (SUV_{max})				^{68}Ga-HBED-PSMA uptake (SUV_{max})			
Cohort	**Patient**	**Parotid**	**Liver**	**Spleen**	**Blood pool**	**Parotid**	**Liver**	**Spleen**	**Blood pool**
A	1	3.0	2.7	2.6	2.6				
	2	3.4	2.3	2.1	2.6				
	3	2.4	2.7	1.8	2.3				
	4	4.1	3.3	2.7	3.0				
	5	2.9	2.4	1.7	3.1				
	6	3.0	2.9	2.6	2.6				
	7	4.4	3.0	3.9	4.5				
	8	3.5	3.0	2.4	2.5				
B	9	5.0	2.6	2.7	1.8	20.0	8.2	9.3	1.8
	10	3.5	4.8	4.8	1.6	18.3	7.2	9.8	1.2
	11	4.4	2.1	2.1	1.7	16.7	4.8	8.8	1.4
	12	3.9	2.2	3.2	1.9	18.7	6.3	15.9	1.7
	13	2.9	2.4	3.2	2.3	14.2	6.2	14.5	1.9
	14	4.2	1.9	1.6	1.9	27.0	5.1	4.4	0.6
Mean		3.6	2.7	2.7	2.5	19.2	6.3	10.5	1.4

Europe PMC Funders Author Manuscripts

Europe PMC Funders Author Manuscripts

Table 3

Absorbed Organ and Whole-Body Doses of ^{68}Ga-THP-PSMA

Organ	Absorbed dose in patient: 1	2	3	4	5	6	7	8	Mean absorbed dose	Median absorbed dose
Adrenal glands	7.00E–03	6.01E–03	7.36E–03	5.02E–03	4.85E–03	5.88E–03	5.57E–03	5.33E–03	5.88E–03	5.72E–03
Brain	1.14E–03	1.31E–03	2.15E–03	1.15E–03	1.20E–03	1.29E–03	9.35E–04	1.47E–03	1.33E–03	1.24E–03
Gallbladder	9.89E–03	7.54E–03	1.11E–02	7.24E–03	9.00E–03	8.42E–03	1.33E–02	7.03E–03	9.20E–03	8.71E–03
Lower large intestine	1.92E–02	8.42E–03	1.32E–02	6.63E–03	1.00E–02	9.39E–03	8.78E–03	1.01E–02	1.07E–02	9.71E–03
Small intestine	1.71E–02	1.44E–02	1.52E–02	2.25E–02	1.53E–02	1.53E–02	1.25E–02	1.36E–02	1.57E–02	1.53E–02
Stomach	9.89E–03	7.85E–03	1.17E–02	7.49E–03	7.84E–03	8.03E–03	7.70E–03	6.86E–03	8.42E–03	7.84E–03
Upper large intestine	8.04E–03	7.46E–03	9.96E–03	6.34E–03	7.36E–03	7.24E–03	6.48E–03	7.16E–03	7.50E–03	7.30E–03
Heart	1.04E–02	1.55E–02	2.80E–02	1.42E–02	1.55E–02	1.62E–02	1.50E–02	1.18E–02	1.58E–02	1.53E–02
Kidneys	7.26E–02	6.05E–02	9.07E–02	8.89E–02	9.13E–02	9.91E–02	5.87E–02	7.60E–02	7.97E–02	8.24E–02
Liver	1.83E–02	1.08E–02	1.79E–02	1.10E–02	1.52E–02	1.11E–02	1.05E–02	1.02E–02	1.31E–02	1.10E–02
Lungs	1.69E–02	1.18E–02	1.85E–02	1.53E–02	1.53E–02	1.56E–02	1.33E–02	1.09E–02	1.47E–02	1.53E–02
Muscle	5.15E–03	4.23E–03	5.69E–03	3.44E–03	4.50E–03	4.43E–03	4.25E–03	4.04E–03	4.47E–03	4.34E–03
Pancreas	9.41E–03	7.19E–03	1.46E–02	9.92E–03	1.30E–02	8.82E–03	8.26E–03	8.60E–03	9.98E–03	9.11E–03
Red marrow	9.86E–03	8.20E–03	1.05E–02	6.87E–03	7.58E–03	7.89E–03	7.57E–03	7.69E–03	8.27E–03	7.79E–03
Osteogenic cells	1.24E–02	1.07E–02	1.35E–02	8.52E–03	8.61E–03	1.00E–02	1.03E–02	9.52E–03	1.04E–02	1.02E–02
Skin	4.56E–03	4.13E–03	4.55E–03	2.93E–03	2.79E–03	3.65E–03	3.70E–03	3.56E–03	3.73E–03	3.68E–03
Spleen	1.56E–02	1.14E–02	1.63E–02	1.47E–02	1.38E–02	1.32E–02	1.05E–02	9.65E–03	1.31E–02	1.35E–02
Testes	1.12E–02	9.65E–03	1.08E–02	1.05E–02	1.28E–02	1.12E–02	1.03E–02	9.91E–03	1.08E–02	1.06E–02
Thymus	5.48E–03	4.91E–03	5.73E–03	3.56E–03	3.10E–03	4.31E–03	4.48E–03	4.02E–03	4.45E–03	4.39E–03
Thyroid	8.34E–03	8.07E–03	1.12E–02	6.05E–03	6.93E–03	6.27E–03	7.57E–03	7.38E–03	7.72E–03	7.47E–03
Urinary bladder	1.80E–01	1.78E–01	1.22E–01	1.51E–01	4.50E–01	2.67E–01	1.36E–01	3.36E–01	2.27E–01	1.79E–01
Remainder	7.97E–03	6.80E–03	8.33E–03	5.64E–03	6.28E–03	6.80E–03	6.35E–03	6.38E–03	6.82E–03	6.59E–03
Effective dose (mSv/MBq)	2.05E–02	1.71E–02	1.75E–02	1.60E–02	3.21E–02	2.25E–02	1.52E–02	2.49E–02	2.07E–02	1.90E–02

Europe PMC Funders Author Manuscripts

Europe PMC Funders Author Manuscripts

Table 4
Number of PSMA-Avid Metastatic Lesions Identified

Patient	Gleason score	PSA (μg/L)	No. of lesions									
			Prostate bed (T)		Regional nodes (N)		Nonregional nodes (M1a)		Bone metastases (M1b)		Visceral metastases (M1c)	
			THP	HBED	THP	HBED	THP	HBED	THP	HBED	THP	HBED
9	3 + 4 = 7	2.1	0	0	0	0	0	0	1	1	0	0
10	3 + 3 = 6	14.9	0	0	2	2	1	1	0	0	0	0
11	4 + 4 = 8	50.7	0	0	0	0	10	10	>20	>20	0	0
12	4 + 4 = 8	3.2	0	0	1	1	0	0	0	0	0	0
13	5 + 4 = 9	3	1	1	6	6	0	0	0	0	0	0
14	3 + 3 = 6	8	0	1	2	3	0	0	0	0	0	0